An Infrared Reflection−Absorption Spectroscopy Study of the Secondary Structure in $(KL_4)_4K$, a Therapeutic Agent for Respiratory Distress Syndrome, in Aqueous Monolayers with Phospholipids†

Peng Cai, Carol R. Flach, and Richard Mendelsohn*

Department of Chemistry, Newark College of Arts and Sciences, Rutgers University, 73 Warren Street, Newark, New Jersey 07102

Received February 28, 2003; Revised Manuscript Received June 6, 2003

ABSTRACT: KLLLLKLLLLKLLLLKLLLLK (KL_4) has been suggested to mimic some aspects of the pulmonary surfactant protein SP-B and has been tested clinically as a therapeutic agent for respiratory distress syndrome in premature infants [Cochrane, C. G., and Revak, S. D. (1991) *Science 254*, 566−568]. It is of obvious interest to understand the mechanism of KL_4 function as a guide for design of improved therapeutic agents. Attenuated total reflection (ATR) IR measurements have indicated that KL_4 is predominantly α-helical with a transmembrane orientation in lipid multilayers (*1*), a geometry quite different from the originally proposed peripheral membrane lipid interaction. However, the lipid multilayer model required for ATR may not be the best experimental paradigm to mimic the in vivo function of KL_4. In the current experiments, IR reflection−absorption spectroscopy (IRRAS) was used to evaluate peptide secondary structure in monolayers at the air/water interface, the physical state that best approximates the alveolar lining. In contrast to the ATR−IR results, KL_4 (2.5−5 mol %) films with either DPPC or DPPC/DPPG (7/3 mol ratio) adopted an antiparallel β-sheet structure at all surface pressures studied ≥5 mN/m, including pressures physiologically relevant for lung function (40−72 mN/m). In contrast, in DPPG/KL_4 films, the dominant conformation was the α-helix over the entire pressure range, a possible consequence of enhanced electrostatic interactions. IRRAS has thus provided unique molecular structure information and insight into KL_4/lipid interaction in a physiologically relevant state. A structural model is proposed for the response of the peptide to surface pressure changes.

Pulmonary surfactant, a thin lipid−protein film coating the alveolar/air interface of the mammalian lung, functions in vivo to lower surface tension, thereby reducing the work of breathing. Surfactant deficiency results in respiratory distress syndrome (RDS)[1] in premature infants while pathological alterations result in the adult version of the disease (ARDS). The mechanism by which surfactant lowers surface tension is the goal of intensive current study with a plethora of molecular, biophysical, and ultrastructural techniques. Surfactant in vivo must possess two apparently contradictory attributes. It must be able to form stable films at the high surface pressures (∼70 mN/m) that develop upon exhalation; it must also be able to spread sufficiently rapidly across the air/alveolar interface to keep up with breathing rates.

The primary chemical constituents of surfactant are lipids (mostly phospholipids) and proteins (*2*). Among the former, the main constituent is 1,2-dipalmitoylphosphatidylcholine (DPPC), which constitutes ∼40 mol % of the material. In multilayer preparations (bilayers, vesicles, etc.), DPPC exists in an ordered (gel) phase at physiological temperatures. In monolayers, DPPC is the major surfactant constituent that can form stable monolayers at 70 mN/m under compressive forces. However, DPPC spreads far too slowly in vivo to be effective as a therapeutic agent.

Surfactant proteins account for 5−10% of total surfactant composition by weight. They confer important biophysical and regulatory properties on surfactant. Two small, hydrophobic, surface-active proteins, SP-B and SP-C, have been shown to accelerate the spreading of DPPC across an air/water interface (*3*). SP-B promotes rapid insertion of phospholipids into aqueous monolayers and induces formation of tubular myelin, the unusual form of surfactant that facilitates its delivery into the air/alveolar lining. The importance of SP-B has been emphasized through the studies of Lin et al. (*4*), who showed that knockout of the SP-B gene in mice proved to be a lethal mutation.

SP-B is a 17.4 kDa homodimer in which each subunit contains three intrachain disulfides. A single intermolecular disulfide bond generates the putatively active homodimer. The molecule is rich in cationic and hydrophobic amino acids. CD spectroscopy has shown that porcine SP-B is 40−60% α-helical with 15% β-sheet secondary structure. SP-B is suggested to contain four amphipathic helical segments oriented pairwise in an antiparallel fashion. This

† This work was supported by USPHS Grant GM 29864 to R.M.

* To whom correspondence should be addressed. Phone: (973) 353-5613. Fax: (973) 353-1264. E-mail: mendelso@andromeda.rutgers.edu.

[1] Abbreviations: ARDS, adult RDS; KL_4, peptide KLLLLKLLLLKLLLLKLLLLK; ATR, attenuated total reflection; A/W, air/water; CD, circular dichroism; DPPC, 1,2-dipalmitoylphosphatidylcholine; DPPG, 1,2-dipalmitoylphosphatidylglycerol; HPLC, high-pressure liquid chromatography; IRRAS, infrared reflection−absorption spectroscopy; POPG, 1-palmitoyl-2-oleoylphosphatidylglycerol; RA, reflectance−absorbance; RDS, respiratory distress syndrome; SP-B, surfactant protein B; π, surface pressure.

10.1021/bi030052b CCC: $25.00
Published on Web 07/15/2003

arrangement is proposed to present a hydrophobic face available for slight penetration into the lipid acyl chain region with the more polar surface remaining in the bilayer periphery. Fluorescence measurements are consistent with this and have led to the suggestion that SP-B orders the bilayer surface of model membranes but has little effect on the hydrophobic interior (*5*). Although many bulk phase studies of SP-B structure and its interaction with lipids have appeared, the majority of monolayer studies have been limited to microscopic techniques, where molecular structure information is not available. In an important contribution, Krol et al. (*6*) used scanning force microscopy to study DPPC/DPPG/SP-B monolayers and observed disklike protrusions at surface pressures of 50−54 mN/m.

Synthetic surfactant peptides based on patterns of structure or charge found in the human SP-B or SP-C appear to mimic some of the structural and functional properties of the native proteins and thus may offer a useful basis for the design of synthetic agents for therapeutic intervention. Toward this end, Cochrane and co-workers (*7*) suggested that the simple peptide KLLLLKLLLLKLLLLKLLLLK (KL_4) with its pattern of five positively charged lysine residues interspaced with four leucines would be an effective therapeutic agent as it may mimic aspects of the positive charge and hydrophobic residue distribution in SP-B. This peptide indeed induced permanent normal pulmonary function in preterm human infants in a phase 2 clinical study (*8*). Despite this success, the peptide demonstrated mixed results in several animal model systems (*9*, *10*).

To model the lipid/peptide interaction, Cochrane et al. (*7*) proposed that KL_4 mimics the action of SP-B suggested from earlier fluorescence experiments where the lysine residues were suggested to interact with the polar headgroups. It was also suggested that the leucine side chains penetrated into the hydrophobic regions. This model predicts a particular structure and/or orientation for the peptide in lipid environments. Gustafsson et al. (*1*) evaluated both secondary structure and peptide orientation in bulk phases with CD and ATR−IR measurements. Their measurements did not support Cochrane's proposal and suggested that KL4 forms a helix oriented parallel to the lipid acyl chains. It is not entirely clear how to reconcile the ATR observation of helices parallel to the acyl chains with the fact that the lysine residues (in a helical wheel representation) in KL_4 are evenly distributed over the entire helical circumference, assuming the peptides to be dispersed as monomers into the bilayers.

The current study uses infrared reflection−absorption spectroscopy (IRRAS) to directly monitor the secondary structure of KL_4 in lipid monolayers at the air/water (A/W) interface with DPPC or 1,2-dipalmitoylphosphatidylglycerol (DPPG) along with ternary mixtures of KL_4 with DPPC/DPPG. These lipids, alone and in combination, are widely used as surfactant mimics. IRRAS is currently the only physical method able to directly monitor peptide secondary structure in situ in Langmuir films. The primary rationale for this experiment is that design of therapeutic agents for RDS and ARDS will be advanced if a molecular level understanding of those factors which control surfactant spreading at the air/alveolar interface is achieved. Toward this end, it is essential to monitor the secondary structure and, if possible, the orientation of the putative agent in surface films. The current experiments indicate that KL_4 secondary structure in lipid monolayers strongly depends on lipid composition, charge, and surface pressure. These results cannot be anticipated from bulk phase experiments.

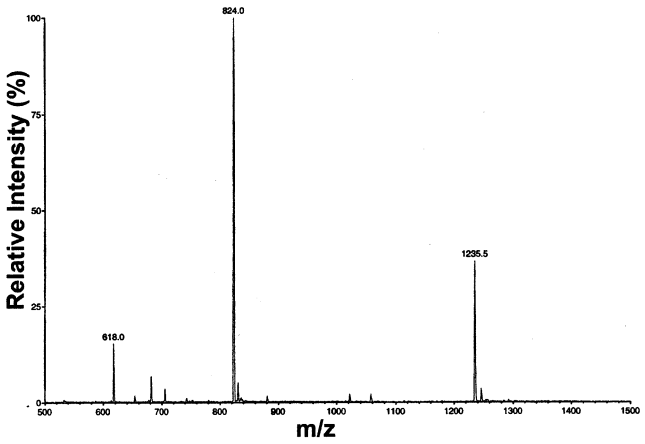

FIGURE 1: Electrospray ionization mass spectrum of purified KL_4 peptide.

EXPERIMENTAL PROCEDURES

Materials. DPPC and DPPG were purchased from Avanti Polar Lipids (Alabaster, AL). Chloroform, methanol, and EDTA were obtained from Fisher Scientific (Pittsburgh, PA). Tris-HCl [tris(hydroxymethyl)aminomethane hydrochloride], Trizma [tris(hydroxymethyl)aminomethane base], and sodium chloride were purchased from Sigma (St. Louis, MO). D_2O with 99.9% isotopic enrichment was purchased from Cambridge Isotope Laboratories (Andover, MA). The crude KL_4 peptide was custom synthesized by Biopeptide Co. (San Diego, CA) with a purity of ∼85% by HPLC. This crude KL_4 was further purified by reverse-phase HPLC using a YMC ODS-AL semipreparative column (Millford, MA) with an eluent gradient of water/acetonitrile, both containing 0.1% TFA. The identity and purity of the chromatographed KL_4 peptide were confirmed by electrospray ionization mass spectrometry and HPLC, respectively. The mass spectrum showed only one major component having a molecular weight consistent with KL_4 (Figure 1), and the HPLC assay revealed a purity of greater than 98%.

Monolayer Sample Preparation and IRRAS Measurements. A stock DPPC solution was prepared in chloroform at 2.0 mg/mL, a stock DPPG solution was prepared in chloroform/methanol (10/1 v/v) at 1.9 mg/mL, and a stock KL_4 peptide solution was prepared in chloroform/methanol (1/1 v/v) at 0.54 mg/mL. The sample solutions were prepared by mixing the stock solutions in various proportions to obtain the desired lipid/peptide ratio.

IRRAS spectra were acquired with a Bruker Instruments Equinox 55 spectrometer equipped with an external variable angle reflectance accessory, the XA511. The accessory is coupled to a custom-designed Langmuir trough constructed by Nima Technology Ltd. (Coventry, England) equipped with a Nima model PS4 surface pressure sensor. The instrument has been described elsewhere (*11*). Briefly, the IR beam is directed through the external port in the spectrometer and is reflected by three mirrors in a rigid mount prior to being focused on the water surface. Computer-driven stepper motors rotate the mirrors to obtain the desired angle of incidence. A wire grid polarizer is placed into the optical

path directly before the beam impinges on the water surface. The reflected light is collected at the same angle as the angle of incidence, follows an equivalent mirror path, and is directed onto a narrow-band mercury cadmium telluride detector. The entire experimental setup is enclosed and purged to keep the relative humidity levels both low and as constant as feasible.

A D_2O-based subphase consisting of 100 mM NaCl and 0.1 mM EDTA in 5 mM Tris buffer at pD 7 was used for all IRRAS experiments. A D_2O-based subphase is used to eliminate the reflectance−absorbance (RA) from the (liquid) H_2O bending vibration and to lessen the absorbance from the rotation−vibration bands of water vapor, both of which occur in the conformation-sensitive amide I region. The subphase temperature was thermostated at 21.0 ± 0.5 °C. Aliquots of the sample solutions (3−5 μL) were spread dropwise on a clean surface (maximum surface area of ∼86 cm^2). A minimum of 40 min was allowed for solvent evaporation and film relaxation/equilibration prior to compression. All samples were spread with initial pressure values (which varied depending on the final pressure desired) from 0 to ∼13 mN/m, and π−*A* isotherms were acquired during intermittent compression. IRRAS spectral acquisition was conducted 5 min after the stopping of the barrier at the desired surface pressure. The surface pressure drop during IRRAS measurements was <3 mN/m in high-pressure regions and <1 mN/m in low-pressure regions.

Interferograms were collected with the use of a sample shuttle program to compensate for the residual water vapor rotation−vibration bands in the amide I region. A total of 1024 scans were acquired at ∼8 cm^{-1} resolution, in 4 blocks of 256 scans each, co-added, apodized with a Blackman−Harris 3-term function, and fast Fourier transformed with two levels of zero filling to produce spectral data encoded at ∼2 cm^{-1} intervals. Spectra were acquired using both p-polarized and s-polarized radiation at a 40° and 50° angle of incidence, respectively.

IRRAS Data Analysis. Data analysis was performed using Grams/32 software (Galactic Industries Corp., Salem, NH). Spectra are presented after baseline correction. The excellent spectral quality and compensation of water vapor precluded the need for water vapor subtraction. IRRAS spectra of the amide I region were curve-fit using two Gaussian bands. The position of the first band was fixed at 1652 ± 5 cm^{-1} with a full width at half-height of 30 cm^{-1}, and the second band was located at 1620 ± 5 cm^{-1} with a 20 cm^{-1} width. Ratios of curve-fit areas are presented since extinction coefficients for various peptide secondary structures have not been extensively reported and the orientation of secondary structure elements within the peptide at the A/W interface is unknown. Recently, anisotropic optical constants were reported for polypeptides of known secondary structure where the total integrated extinction coefficient for the amide I mode of an α-helix was essentially the same as that found for an antiparallel β-sheet (*12*).

RESULTS

IRRAS spectra in the region of 1550−1800 cm^{-1} acquired from aqueous monolayers of DPPC containing KL_4 (20/1 lipid/peptide mol ratio) on D_2O at several surface pressures (π) are shown in Figure 2. This film was spread with an initial pressure value of 0 mN/m. The spectral region shows the lipid C═O stretching (1700−1750 cm^{-1}) and the amide I (peptide bond C═O stretching, 1615−1695 cm^{-1}) vibrations. The latter are well-known for their sensitivity to peptide or protein secondary structure.

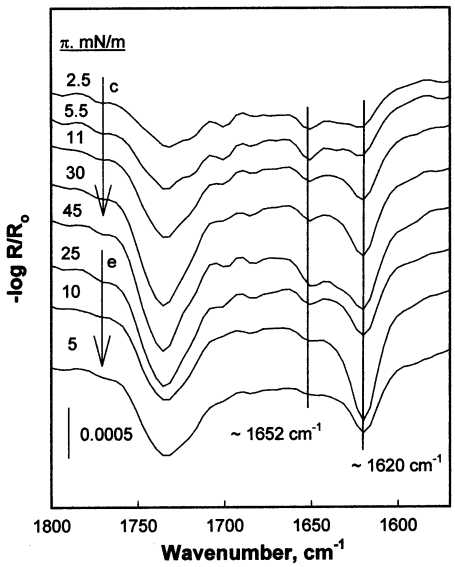

FIGURE 2: IRRAS spectra of the lipid carbonyl and peptide amide I region (1550−1800 cm^{-1}) for a mixed film of DPPC with 5 mol % KL_4 on a D_2O subphase. Spectra were acquired using s-polarization, and surface pressure values are noted from top to bottom during compression (c) and expansion (e) of the film. The angle of incidence was 50°.

At π = 2.5 mN/m, the amide I mode consists of two major components. The first constituent at ∼1652 cm^{-1} is assigned, in accordance with many literature assignments, to α-helical secondary structure. The major component near 1620 cm^{-1} is assigned to an extended structure, possibly arising from an antiparallel β-sheet. A similar spectral pattern is observed at π = 5.5 mN/m. As π is increased toward 45 mN/m, the intensity of the β-sheet marker band relative to the α-helical marker band increases. Expansion of the film from 45 to 5 mN/m shows the α-helix ⇒ β-sheet interconversion to be irreversible. In fact, it appears that the relative intensity of the helix marker band continues to diminish slightly upon expansion, suggesting that a process under kinetic control is contributing to the interconversion. IRRAS spectra of pure KL_4 peptide monolayers acquired over a range of surface pressure values (0−17 mN/m, not shown) are consistent with an antiparallel β-sheet assignment due to the presence of both the dominant amide I component at 1620 cm^{-1} and the weaker ∼1690 cm^{-1} marker band.

The pressure-dependent structural transition for the DPPC/KL_4 monolayer is clearly displayed in Figure 3A, where the fraction of the total amide I band area due to the 1652 cm^{-1} component is shown as a function of surface pressure for compression and subsequent expansion of a DPPC/KL_4 monolayer. The percentage of the total amide I band area assigned to the α-helical component is observed to decrease from ∼40% to 20% upon compression with a further decrease to ∼10% upon expansion. Curve-fit band areas as described in Experimental Procedures were used to generate the ratios shown in Figure 3.

The spectra shown in Figure 2 were acquired with s-polarized radiation. To evaluate whether the observed

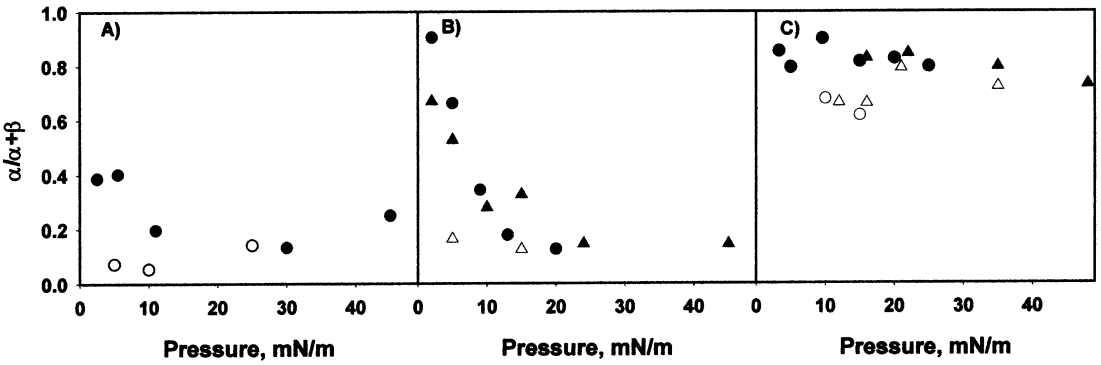

FIGURE 3: Peak area ratio of amide I band intensities for 1652/(1652 + 1620) cm^{-1} as a function of surface pressure during intermittent compression (filled symbols) and expansion (open symbols), as obtained from curve fitting. 1652 cm^{-1} is assigned to the α-helical secondary structure; 1620 cm^{-1} is assigned to extended forms, including the antiparallel β-sheet. (A) DPPC with 5 mol % KL_4 over a pressure range of 2.5−45 mN/m. (B) DPPC/DPPG, 7/3 (mol ratio), with 2.5 mol % KL_4 over a pressure range from 2 to 45 mN/m (triangles) and with 5 mol % KL_4 over a pressure range from 0 to 20 mN/m (circles). (C) DPPG with 5 mol % KL_4 over a pressure range from 3.3 to 25 mN/m (circles) and at a pressure range from 16 to 48 mN/m (triangles).

intensity changes in the amide I contour may arise from orientation changes in the peptide rather than changes in the secondary structure, IRRAS spectra were acquired with p-polarized radiation (data not shown). These exhibited the same patterns of intensity alteration as seen in the s-polarized spectra. As we have noted in detail elsewhere, this observation eliminates the possibility that orientation changes are responsible for the spectral changes (*13*). Thus as π is increased, the predominant secondary structure adopted by KL_4 is that of an antiparallel β-sheet. This conformation is retained at physiologically relevant pressures (>40 mN/m).

To explore KL_4 secondary structure in a lipid environment more relevant to surfactant, we examined the peptide in aqueous monolayers of DPPC/DPPG (7/3 mol/mol) in both 40/1 and 20/1 total lipid/peptide mol ratios. The spectra, displayed in panels A and B of Figure 4, respectively, show the same progression of relative amide I constituent band intensities as each monolayer, spread at an initial surface pressure of 0 mN/m, is compressed. It is noted that exceptional signal to noise ratios were achieved in the data for the 40/1 total lipid/KL_4 mol ratio (Figure 4A). The ratio of the area for the 1652 cm^{-1} component is plotted as a fraction of total amide I band area in Figure 3B. It is interesting to note that the percentage of amide I intensity attributed to helical structure is approximately the same (over the pressure range shown in Figure 3B) for both peptide concentrations. Comparing panel A of Figure 3 to panel B at $\pi \leq 5$ mN/m, it is evident that a greater percentage of helix is present in the DPPC/DPPG/peptide monolayers compared to the DPPC/peptide film during initial compression. At higher pressure values, however, the relative amount of helix is comparable in the two different lipid films, and the percentage remains approximately the same (<20% helical component) upon subsequent expansion. Thus, KL_4 initially adopts mixed α-helical/β-sheet secondary structure, which irreversibly interconverts to a β-sheet form as π is increased in both DPPC and DPPC/DPPG monolayers.

The observation of β-sheet secondary structure was not anticipated on the basis of the reported IR experiments in DPPC/DPPG (7/3) bilayers, in which α-helical secondary structure dominated (*1*). It thus seemed appropriate to evaluate the effects of electrostatics on lipid/KL_4 interaction. IRRAS data were acquired from DPPG/KL_4 (20/1) binary films. The 1550−1800 cm^{-1} region of the IRRAS spectrum is displayed over a range of π's in panels A and B of Figure 5 using s- and p-polarized radiation, respectively. Similar pressure-induced changes are observed for both polarizations, indicating that secondary structure transitions as opposed to orientation changes are responsible for the majority of the intensity variation (*13*). Although the signal to noise ratio in the spectra acquired using p-polarized radiation is not as high as that obtained using s-polarization, it is evident in both spectra at $\pi = 3.3$ mN/m that the band at ~1652 cm^{-1} arising from α-helical structures dominates the amide I contour. As π is increased, and in marked contrast to the behavior in the binary lipid/peptide and DPPC/peptide systems, this feature remains the strongest in every spectrum, although a feature arising from β-sheet forms appears with increasing intensity so that, at a pressure of 25 mN/m, a significant shoulder is present at ~1620 cm^{-1}. The relative intensity of the β-sheet component continues to increase slightly upon expansion of the film from 25 mN/m to lower pressures. Figure 3C clearly illustrates these trends where the band area of the helical component does not drop below 60% of the total amide I area, and the differences between DPPG/KL_4 and the two other lipid/peptide systems are readily distinguished (Figure 3A,B).

To evaluate KL_4 secondary structure at physiologically more relevant pressures, it was necessary to spread DPPG/peptide films at somewhat higher initial pressures. The results are shown in Figure 6 where the film was spread to an initial pressure of 13 mN/m. At all pressures during the compression from 16 to 48 mN/m, the α-helical amide I band component was observed to be the most intense in this region of the IRRAS spectrum. As with the other lipid/peptide systems when a previously compressed film was expanded from its highest pressure, the increased area/molecule produced an increase in the β-sheet conformation marker band. At physiological pressures, the helical band contributed much more intensity to the amide I contour than in either the pure DPPC lipid monolayer or the 7/3 (DPPC/DPPG) system.

DISCUSSION

The present study was motivated by two factors. First, as KL_4 has been used in clinical trials for pathological states

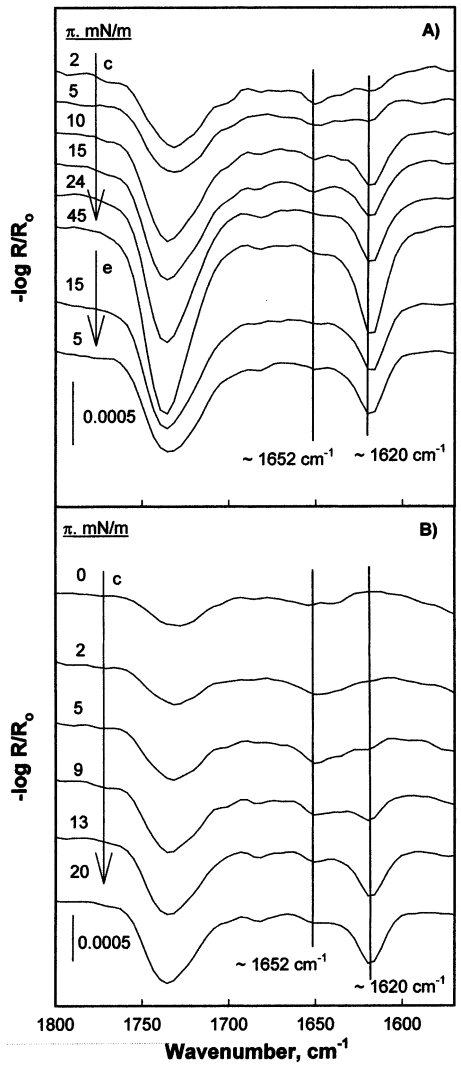

FIGURE 4: (A) IRRAS spectra of the lipid carbonyl and peptide amide I region (1550−1800 cm^{-1}) for a mixed film of DPPC/DPPG, 7/3 (mol ratio), with 2.5 mol % KL_4 on a D_2O subphase. Spectra were acquired using s-polarization, and surface pressure values are noted from top to bottom during compression (c) and expansion (e) of the film. The angle of incidence was 50°. (B) IRRAS spectra of the lipid carbonyl and peptide amide I region (1550−1800 cm^{-1}) for a mixed film of DPPC/DPPG, 7/3 (mol ratio), with 5 mol % KL_4 on a D_2O subphase. Spectra were acquired using s-polarization, and surface pressure values are noted from top to bottom during compression (c) of the film. The angle of incidence was 50°.

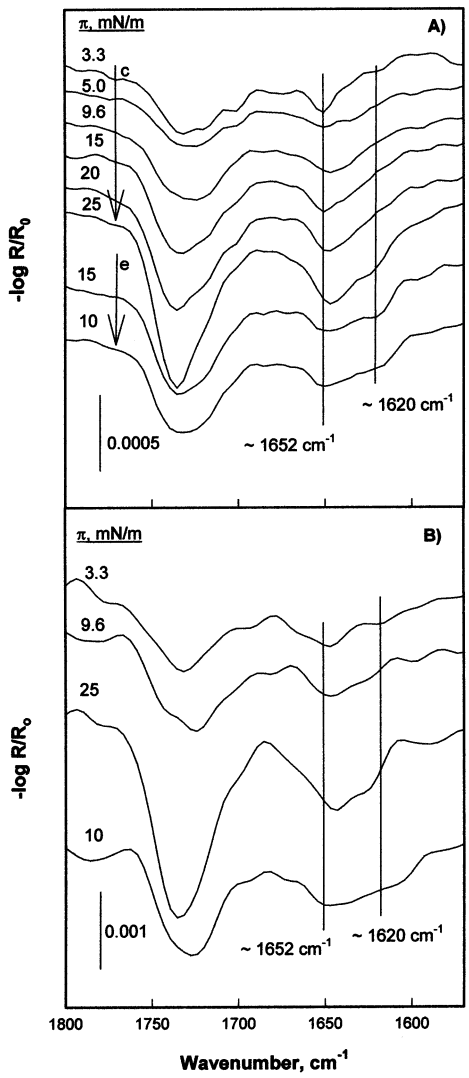

FIGURE 5: (A) IRRAS spectra of the lipid carbonyl and peptide amide I region (1550−1800 cm^{-1}) for a mixed film of DPPG with 5 mol % KL_4 on a D_2O subphase over a pressure range of 3.3−25 mN/m. Spectra were acquired using s-polarization, and surface pressure values are noted from top to bottom during compression (c) and expansion (e) of the film. The angle of incidence was 50°. (B) IRRAS spectra of the lipid carbonyl and peptide amide I region (1550−1800 cm^{-1}) for a mixed film of DPPG with 5 mol % KL_4 on a D_2O subphase. Spectra were acquired using p-polarization, and surface pressure values are noted from top to bottom during compression and expansion of the film. The angle of incidence was 40°.

of the lung in both animal models and in humans, it seemed of importance to determine the secondary structures adopted by this peptide in monolayers in situ at the air/water interface. These experiments are clearly necessary to begin to understand the molecular mechanism of KL_4 action and to design improved versions of the molecule.

Current structural models for KL_4/lipid interaction are not without controversy. The initial structural suggestions of Cochrane and Revak (*7*) have apparently been refuted to some extent by the ATR−IR studies of Gustafsson et al. (*1*) as discussed in the introduction. However, as noted by Cochrane (*9*), the latter were carried out in a multilayer environment, not entirely appropriate for the surfactant system (see below for comments about the possible involvement of multilayers in the respreading of surfactant). It is necessary to bring an independent method to bear on the problem, in this instance IRRAS, which can measure peptide secondary structure under physiologically relevant conditions.

The current IRRAS results provide a direct measurement of KL_4 secondary structure in monolayers at the A/W interface. The secondary structures adopted by the peptide are evidently a function of lipid headgroup charge and surface pressure. In both DPPC and 7/3 DPPC/DPPG mixtures, KL_4 adopted (at surface pressures >40mN/m, appropriate for the physiological state of the lung) a predominantly antiparallel β-sheet secondary structure. Within the limited concentration range (2.5−5 mol % peptide) studied here, this effect was independent of the lipid/protein ratio. This observation is quite different from the result of Gustafsson et al. (*1*), who observed helical forms in their ATR−IR studies. Their studies were carried out at a lipid composition and lipid/

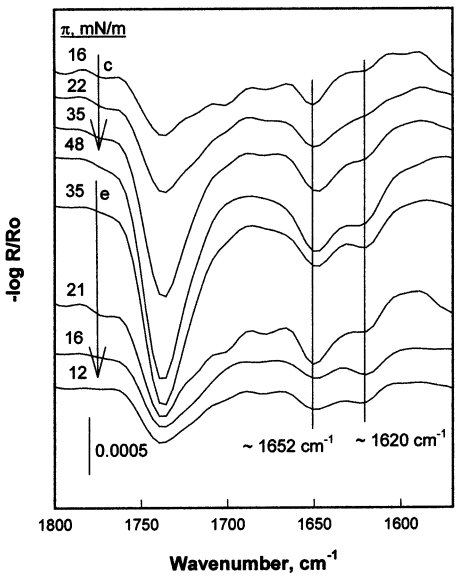

FIGURE 6: IRRAS spectra of the lipid carbonyl and peptide amide I region (1550−1800 cm^{-1}) for a mixed film of DPPG with 5 mol % KL_4 on a D_2O subphase over a pressure range of 16−48 mN/m. Spectra were acquired using s-polarization, and surface pressure values are noted from top to bottom during compression (c) and expansion (e) of the film. The angle of incidence was 50°.

peptide mol ratio quite similar to the current measurements at 2.5 mol %. The differences between the two studies may then be dependent on the different physical states adopted by the lipid preparations, i.e., multilayers on an ATR crystal versus monolayers at the A/W interface. Obviously, many factors may differ between the two experimental approaches. Perhaps most important is the difference in the hydrophobic thickness in the two preparations. But, not to be overlooked is the fact that multilayers are thought to possess a surface pressure equivalent to monolayers at 32 mN/m (*14*). If this is the case, the high effective surface pressure may prevent KL_4 from adopting a thermodynamically preferred secondary structure or from inserting into the lipid bilayer. The close apposition of lipid bilayers imposed by the multilayer structure is likely to influence the conformation of KL_4 as well.

The IRRAS experiment permits much more flexibility in this regard compared to ATR. The important variable of surface pressure may be controlled and extended into the physiologically relevant range. Although the monolayers are spread at low initial pressure where the lipid is in the liquid expanded state (disordered acyl chains), as pressure is increased, the chains become conformationally ordered. It must be noted that the formation of the β-sheet forms is not an artifact of the IRRAS experiment. This is clearly revealed from the data for DPPG/KL_4, in which helical secondary structure is the dominant conformation at all pressures.

The primary observation from this work is that the presence of significant levels of zwitterionic DPPC imposes an extended structure on KL_4, at surface pressures approaching those in the lung. However, at high levels of DPPG, the peptide retains a majority of α-helical secondary structure as adopted in the bulk phase.

Many years ago, Clements (*15*) proposed that at high pressures the stability of the film required a process by which the surface concentration of DPPC was enhanced. The process, not defined in molecular structure terms, was termed "squeeze-out" and alluded to a concentrating of the DPPC in the surface film upon compression. About 10 years ago, we observed this phenomenon at high pressures in binary lipid mixtures such as DPPC/POPG (*16*). The deficiency in the model as then propounded was that the mechanism of respreading surfactant was not defined.

Toward this end, several recent studies have aimed at determining the physical state (monolayer or otherwise) of surfactant in the lung. Recent data, both on intact lung and on transferred films, have suggested that multilayers form at high π values during expansion−contraction cycles. Schürch et al. (*17*) used electron microscopy to observe the formation of multilayer structures in guinea pig lung with variations in the number of lamellae from 2 to 7. To characterize similar structures in surface films formed from synthetic phospholipids and peptides, von Nahmen et al. (*18*) used fluorescence microscopy to directly search for multilayers at high pressures in DPPC/DPPG films in the presence and absence of SP-C. Multilayers were indeed observed in the late stages of compression. SP-C facilitated formation of these structures. Recently, Takamoto et al. (*19*) noted that SP-B and SP-C induced a two- to three-dimensional transformation of the fluid phase fraction in mixed DPPG/POPG monolayers and, further, that SP-B induced a reversible folding transition at monolayer collapse, allowing all components of surfactant to remain near the interface. These recent observations lead to the suggestion that multilayers may form a reservoir from which respreading is facilitated. Thus, both monolayers and multilayers may play a role in the function of the surfactant film during compression−expansion cycles.

The current result leads to the following suggestion for a mechanism of KL_4 action. At low surface pressures, DPPC and DPPG, or some of the other negatively charged constituents of the native surface film, are presumably reasonably well mixed in the monolayers. KL_4 would initially adopt an extended conformation, most likely at the aqueous surface or interfacial region of the lipid monolayer. The location of the peptide with respect to the monolayer is inferred from the distribution of positive charge (Lys residues) above and below the plane of the sheet. Upon compression (in the native system) multilayer structures would form. The multilayers would be enriched in the PG component of the surfactant, and the peptide would adopt the helical secondary structure as observed in the current experiments in the presence of DPPG. Recently reported IRRAS results indicate that at physiological concentrations of SP-B/C preferential interactions take place between DPPG and the proteins in DPPC/DPPG (7/1) monolayers (*20*). In that report, acyl chain order in DPPG is increased during compression at lower pressures, suggesting that the proteins preferentially interact with the anionic lipid headgroup and that some degree of lipid phase separation is taking place. As stated in the introduction, the dispersion of charged Lys residues around the circumference of the helix is likely to inhibit insertion of the peptide into the hydrophobic interior of the bilayer. The results from the current experiments are meshed with those of Schurch et al. (*17*), Van Nahmen et al. (*18*), Takamoto et al. (*19*), and the Münster group (*21*, *22*), who utilized TOF/SIMS and detected multilayer formation in transferred films at relatively high surface pressure. These ideas are summarized in the cartoon in Figure 7. The biological advantage of the

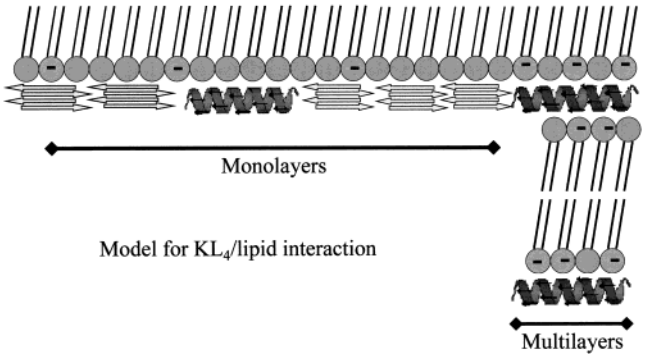

FIGURE 7: Schematic representation of KL_4 peptide secondary structures in the lipid monolayer region at low surface pressure and in multilayers at higher surface pressure upon compression [PG headgroup noted with (−) charge]. Initially, the peptide would enter the interfacial region of the lipid monolayer. Upon compression, the formation of multilayers enriched in the PG component of the surfactant would form. Consequently, the peptide would adopt an α-helical secondary structure. See text for details.

mechanism described above and delineated in Figure 7 may lie in the fact that the presence of helical structures bridging the monolayer to the multilayer and bridging between bilayers within the reservoir may sufficiently perturb the lipid packing to facilitate the structural reorganization that is required to respread the reservoir lipids upon film expansion. The remixing of DPPC with the other lipids upon expansion may induce a helix ⇒ sheet transition with concomitant reformation of the mixed monolayer components as the pressure is lowered from ∼72 to 40 mN/m during the expansion part of the cycle. The model depicted in Figure 7 is partly amenable to testing. IRRAS studies in our laboratory (P. Cai, C. R. Flach, and R. Mendelsohn, manuscript in preparation) used polarized IRRAS and pressure−area isotherms to monitor the orientation of the β-sheet in KL_4 and of the α-helix in the related peptide NH_2-LLLKLLKLLLKLL-KLLKLLL-COOH. At lower pressures in each case (monolayers), both the helix and the β-sheet were oriented preferentially parallel to the aqueous surface, as depicted in the figure.

Conformational flexibility as observed in the current case and in prior studies from this laboratory for SP-B peptides (*23*) has also been observed by Desbat and co-workers in a different context (*24*). They studied the monolayer behavior of membrane lytic peptides of composition L_iK_j ($i = 2j$). Peptides longer than 12 residues adopted an α-helical structure at the A/W interface as expected from their design, while peptides of lengths between 5 and 9 residues formed intermolecular β-sheets. In the current work, a strong dependence of secondary structure on the lipid headgroup charge in monolayers was observed. In previous studies, we synthesized a peptide fragment of SP-B, $SP\text{-}B_{9-36}$, and found an α ↔ β secondary structure transition, reversible with changes in surface pressure. As noted by Castano et al. (*24*), the presence of α-helices is evidently not an essential criterion for the surface activity of proteins or peptides containing alternating charged and hydrophobic residues. We would also note that bulk phase secondary structure information is not necessarily transferable to the A/W interface.

Finally, we suggest that a combination of physical approaches may be useful in testing (in monolayers) some of the structural considerations discussed above. A combination of fluorescence spectroscopy (in situ at the A/W interface) to search for domain formation, along with more sophisticated methods such as the TOF/SIMS approach used by the Munster group to track multilayer formation in transferred films (*21*, *22*), and IRRAS to examine peptide secondary structure and orientation would seem to be an attractive experimental approach. Finally, it is noteworthy that surface biophysical techniques have reached the point where quantitative models for pulmonary surfactant function, based on molecular structure determination and domain formation in monolayers, may be rigorously tested.

ACKNOWLEDGMENT

We thank Prof. Dr. Hans-Joachim Galla for interest and discussions.

REFERENCES

1. Gustafsson, M., Vandenbussche, G., Curstedt, T., Ruysschaert, J. M., and Johansson, J. (1996) *FEBS Lett. 384*, 185−188.
2. Johansson, J., and Curstedt, T. (1997) *Eur. J. Biochem. 244*, 675−693.
3. Pérez-Gil, J., and Keough, K. M. W. (1998) *Biochim. Biophys. Acta 1408*, 203−217.
4. Lin, S., Na, C. L., Akinbi, H. T., Apsley, K. S., Whitsett, J. A., and Weaver, T. E. (1999) *J. Biol. Chem. 274*, 19168−19174.
5. Baatz, J., E., Elledge, B., and Whitsett, J. A. (1990) *Biochemistry 29*, 6714−6720.
6. Krol, S., Ross, M., Sieber, M., Künneke, S., Galla, H.-J., and Janshoff, A. (2000) *Biophys. J. 79*, 904−918.
7. Cochrane, C. G., and Revak, S. D. (1991) *Science 254*, 566−568.
8. Cochrane, C. G., Revak, S. D., Merritt, T. A., Heldt, G. P., Hallman, M., Cunningham, M. D., Easa, D., Pramanik, A., Edwards, D. K., and Alberts, M. S. (1996) *Am. J. Respir. Crit. Care Med. 153*, 404−410.
9. Cochrane, C. G. (1998) *FEBS Lett. 430*, 424.
10. Walther, F. J., Hernández-Juviel, J., Bruni, R., and Waring, A. J. (1997) *Am. J. Respir. Crit. Care Med. 156*, 855−861.
11. Flach, C. R., Xu, Z., Bi, X., Brauner, J. W., and Mendelsohn, R. (2001) *Appl. Spectrosc. 55*, 1060−1066.
12. Buffeteau, T., Le Calvez, E., Castano, S., Desbat, B., Blaudez, D., and Dufourcq, E. J. (2000) *J. Phys. Chem. B 104*, 4537−4544.
13. Bi, X., Flach, C. R., Perez-Gil, J., Plasencia, I., Andreu, D., Oliveira, E., and Mendelsohn, R. (2002) *Biochemistry 41*, 8385−8395.
14. Seelig, A. (1987) *Biochim. Biophys. Acta 899*, 196−204.
15. Goerke, J., and Clements, J. A. (1986) in *Handbook of Physiology*: *The Respiratory System III* (Mackelm, P. T., and Mead, J., Eds.) pp 247−261, American Physiology Society, Washington, DC.
16. Pastrana-Rios, B., Flach, C. R., Brauner, J. W., Mautone, A. J., and Mendelsohn, R. (1994) *Biochemistry 33*, 5121−5127.
17. Schürch, S., Green, F. H. Y., and Bachofen, H. (1998) *Biochim. Biophys. Acta 1408*, 180−202.
18. von Nahmen, A., Schenk, M., Sieber, M., and Amrein, M. (1997) *Biophys. J. 72*, 463−469.
19. Takamoto, D. Y., Lipp, M. M., van Nahmen, A., Lee, K. Y. C., Waring, A. J., and Zasadzinski, J. A. (2001) *Biophys. J. 81*, 153−169.
20. Brockman, J. M., Wang, Z., Notter, R. H., and Dluhy, R. (2003) *Biophys. J. 84*, 326−340.
21. Galla, H.-J., Bourdos, N., von Nahmen, A., Amrein, M., and Sieber, M. (1998) *Thin Solid Films 329*, 632−635.
22. Bourdos, N., Kollmer, F., Benninghoven, A., Ross, M., Siever, M., and Galla, H.-J. (2000) *Biophys. J. 79*, 357−369.
23. Dieudonné, D., Mendelsohn, R., Farid, R. S., and Flach, C. R. (2001) *Biochim. Biophys. Acta 1511*, 99−112.
24. Castano, S., Desbat, B., Laguerre, M., and Dufourcq, J. (1999) *Biochim. Biophys. Acta 1416*, 176−194.

BI030052B